Magnetic compensation in the bimetallic oxalates

Peter Reis,[1,2] Randy S. Fishman,[2] Fernando A. Reboredo,[2] and Juana Moreno[1]
[1]*Physics Department, University of North Dakota, Grand Forks, North Dakota 58202-7129, USA*
[2]*Materials Science and Technology Division, Oak Ridge National Laboratory, Oak Ridge, Tennessee 37831-6065, USA*
(Received 4 April 2008; published 30 May 2008)

Bimetallic oxalates are layered molecule-based magnets with either ferromagnetic or antiferromagnetic interactions between transition metals M(II) and M′(III) on an open-honeycomb lattice. Some Fe(II)Fe(III) bimetallic oxalates exhibit magnetic compensation (MC) at a compensation temperature $T_{comp} \approx 30$ K below the ferrimagnetic transition temperature $T_c \approx 45$ K. To see if MC is possible in other bimetallic oxalates, we construct a theoretical model for bimetallic oxalates that exhibit antiferromagnetic interactions. By varying the M(II) and M′(III) average orbital angular momentum, which can be controlled by the choice of interlayer cations, we find regions of MC in the families M(II)Mn(III) with M=Fe, Co, or Ni and V(II)M′(III) with M′=Cr or V but not in the family M(II)Ru(III) with M=Fe or Cu.

DOI: 10.1103/PhysRevB.77.174433 PACS number(s): 75.50.Xx, 71.70.Ej, 75.10.Dg, 75.30.Gw

One of the most intensively-studied molecule-based magnets, the bimetallic oxalates[1,2] are isostructural layered compounds with the chemical formula $A[M(II)M'(III)(ox)_3]$, where M(II) and M′(III) are transition-metal ions with valences +2 and +3. Coupled by the oxalate molecules ox $=C_2O_4$, M(II) and M′(III) form the open-honeycomb lattice sketched in the inset of Fig. 1. While the organic cation A between the bimetallic layers affects the overall properties of the material, it does not change the sign of the magnetic interactions between M(II) and M′(III), which can be either ferromagnetic or antiferromagnetic (AF) with moments pointing out of the layer.

When the magnetic interactions are AF, the moments on the M(II) and M′(III) sublattices may cancel at a compensation temperature T_{comp} below the ferrimagnetic transition temperature T_c. Magnetic compensation (MC) has been extensively documented in the Fe(II)Fe(III) compounds,[3–7] where it occurs only for certain cations A. Fe(II)Fe(III) compounds that exhibit MC are reported to have higher values of the transition temperature $T_c \approx 45$ K and of the Curie–Weiss constant C, with $T_{comp} \approx 30$ K.[4] In earlier papers,[8] two of us developed a model that explains the appearance of MC in some Fe(II)Fe(III) compounds but not in others. In the present paper, we investigate three families of bimetallic oxalates where the AF interactions permit MC, but MC has not yet been observed. We conclude that MC is possible in the M(II)Mn(III) (M=Fe, Co, or Ni)[9] and V(II)M′(III) (M′=Cr or V)[10] families but not in the M(II)Ru(III) (M=Fe or Cu)[11] family.

Strong experimental evidence indicates that the coupling between layers is not primarily responsible for the magnetic ordering of the bimetallic oxalates. In Fe(II)Fe(III) bimetallic oxalates with $A=N(n\text{-}C_nH_{2n+1})_4$, the separation l between bimetallic layers grows from 8.2 to 10.2 Å, as n increases from 3 to 5.[4] If the magnetic order depended on the coupling between the layers, then T_c would decrease as n increases from 3 to 5 rather than increasing from 35 to 48 K. Perhaps even more compelling is the observation[12,13] that the magnetic $s=1/2$ cation $FeCp_2^*$ (Cp^*=pentamethylcyclopentadienyl) hardly changes the transition temperature and coercive field of a wide range of bimetallic oxalates. Therefore, some mechanism besides interlayer coupling is needed to explain the magnetic ordering of well-separated bimetallic layers. Recent studies of Fe(II)Fe(III) compounds[8] demonstrated that the spin-orbit coupling on the Fe(II) ($3d^6$) sites can produce long-range magnetic order even for isolated two-dimensional layers. On the other hand, the spin-orbit coupling sums to zero on the Fe(III) ($3d^5$) sites.

We now extend that model to treat a more general class of bimetallic oxalates, where the spin-orbit coupling affects both the M(II) and M′(III) moments. As discussed further below, susceptibility measurements[5,9,10] reveal that the orbital angular momentum of many bimetallic oxalates is incompletely quenched. MC occurs if the M(II) or M′(III) ions initially order more rapidly with decreasing temperature, due

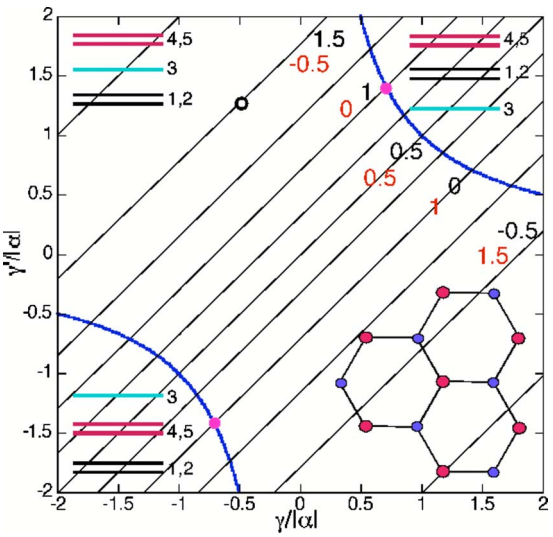

FIG. 1. (Color online) Variation of the orbital angular momentum $\langle L_z \rangle$ of the two doublets due to the crystal-field at the transition-metal ion. The diagonal lines correspond to constant values of $\langle \psi_1 | L_z | \psi_1 \rangle$ (upper-right value) and $\langle \psi_4 | L_z | \psi_4 \rangle$ (lower-left value). Three possible electronic configurations depend on $\gamma/|\alpha|$ and $\gamma'/|\alpha|$. Points of octahedral symmetry are indicated by the two dots, located on the curved boundaries where the singlet and one of the doublets are degenerate. Inset in the lower right is a portion of the open-honeycomb structure of a single bimetallic layer.

to their stronger spin-orbit coupling, than the M′(III) or M(II) ions with the larger saturation moments. So within our model, spin-orbit coupling is responsible for both the two-dimensional order of well-separated layers and the MC within a single bimetallic layer. The cation A can change the magnitude of the spin-orbit coupling, which depends sensitively on the crystal-field potential, but not the sign of the magnetic interaction between M(II) and M′(III), which depends on the overlap between the metal and oxalate wave functions within a single plane. As discussed further below, the spin-orbit interaction is also responsible for the perpendicular magnetic anisotropy of the bimetallic oxalates.

The Hamiltonian for the bimetallic oxalates is assumed to contain three tiers of energies. Because the spin correlations within each $3d$ ion are strong, we assume that Hund's first rule is obeyed. So as confirmed by measurements[9] of the magnetic susceptibility and Curie constant C, the lowest-energy multiplet is in a high-spin state. The crystal-field potential produced by the six oxygen atoms surrounding each $3d$ ion is the next largest energy, inducing a splitting of the $L=2$ multiplet. However, due to the larger spatial extent of their wave functions, $4d$ transition metals such as Ru manifest stronger crystal—field effects that favor a low-spin state.[11] The weakest energies are the AF exchange $J_c\mathbf{S}_2\cdot\mathbf{S}_3$ between the ions and the spin-orbit coupling $\lambda_i\mathbf{L}_i\cdot\mathbf{S}_i$ ($i=2$ or 3) on each metal ion. Also included within this lowest energy scale are contributions to the crystal—field potential that violate C_3 symmetry around the M(II) or M′(III) sites.

Surrounding each M(II) and M′(III) ions are six oxygen atoms that form a heavily-compressed octahedron with C_3 symmetry. Based on symmetry grounds, the crystal-field potential can be expressed as the matrix[8]

$$H^{\mathrm{cf}}=\begin{pmatrix}\gamma & 0 & 0 & \alpha & 0\\ 0 & \gamma' & 0 & 0 & -\alpha\\ 0 & 0 & 0 & 0 & 0\\ \alpha^* & 0 & 0 & \gamma' & 0\\ 0 & -\alpha^* & 0 & 0 & \gamma\end{pmatrix}, \tag{1}$$

where the fivefold degenerate d orbitals are used as the basis and a diagonal matrix has been subtracted. The parameters γ, γ', and α depend on the crystalline field at the M(II) and M′(III) sites, which in turn depends on the positions and ionic states of the surrounding oxygens.

Upon diagonalizing H^{cf}, we obtain two sets of degenerate doublets $|\psi_{1,2}\rangle$ and $|\psi_{4,5}\rangle$ and a singlet $|\psi_3\rangle$.[8] The doublets can be higher or lower in energy than the singlet depending on the crystal-field parameters $\gamma/|\alpha|$ and $\gamma'/|\alpha|$. As shown in Fig. 1, the singlet has the highest energy below the bottom left curve $\gamma\gamma'=-|\alpha|^2$ and the lowest energy above the top right curve $\gamma\gamma'=|\alpha|^2$. It lies between the two doublets in the central region. In addition, Fig. 1 displays lines of constant orbital angular momentum for both doublets: $\langle\psi_1|L_z|\psi_1\rangle$ and $\langle\psi_4|L_z|\psi_4\rangle=1-\langle\psi_1|L_z|\psi_1\rangle$, both of which only depend on the ratio $(\gamma-\gamma')/|\alpha|$.[8] For example, the black circle in Fig. 1 located at $\gamma/|\alpha|=-0.5$ and $\gamma'/|\alpha|=1.25$ corresponds to the values $\langle\psi_1|L_z|\psi_1\rangle=1.5$ and $\langle\psi_4|L_z|\psi_4\rangle=-0.5$. Due to time-reversal symmetry, $\langle\psi_2|L_z|\psi_2\rangle=-\langle\psi_1|L_z|\psi_1\rangle$ and $\langle\psi_5|L_z|\psi_5\rangle=-\langle\psi_4|L_z|\psi_4\rangle$ within each doublet.

TABLE I. Electronic configuration, spin, and spin-orbit coupling constants[15] for M(II) and M(III) transition-metal ions

Ion	n	S	λ[meV]
V^{3+}	$3d^2$	1	12.89
Cr^{3+}	$3d^3$	3/2	11.28
V^{2+}	$3d^3$	3/2	6.94
Mn^{3+}	$3d^4$	2	10.91
Fe^{2+}	$3d^6$	2	−12.64
Co^{2+}	$3d^7$	3/2	−21.94
Ni^{2+}	$3d^8$	1	−40.29
Cu^{2+}	$3d^9$	1/2	−102.78
Ru^{3+}	$4d^5$	1/2 (low spin)	116.54

The occupation of the crystal-field levels is assumed to follow Hund's first rule and the Aufbau principle with the $L=2$ levels filling independently.[14] The orbital configurations, spins, and spin-orbit coupling constants λ [15] for the transition metals studied in this paper are summarized in Table I. Using mean-field (MF) theory to treat the exchange interaction $J_c\mathbf{S}_2\cdot\mathbf{S}_3$, the Hamiltonians on the M(II) and M′(III) sites can be written

$$H_2=\lambda_2\mathbf{L}_2\cdot\mathbf{S}_2+3J_c\langle S_{3z}\rangle S_{2z}, \tag{2}$$

$$H_3=\lambda_3\mathbf{L}_3\cdot\mathbf{S}_3+3J_c\langle S_{2z}\rangle S_{3z}. \tag{3}$$

The spin-orbit and exchange interactions are assumed to be much smaller than the crystal-field splittings. Therefore, each Hamiltonian can be restricted to a configuration where one doublet, carrying an average orbital angular momentum L_2 or L_3, is occupied by an odd number of electrons. We can treat the case where each doublet is occupied by an even number of electrons by setting L_2 or L_3 to zero. Of course, $\langle\mathbf{L}_i\rangle$ is the only nonzero along the z direction perpendicular to the bimetallic planes.

To demonstrate this approach, consider again the black circle in Fig. 1. For a Mn(III) ($3d^4$) ion with these crystal-field parameters, the upper doublet $|\psi_{4,5}\rangle$ would contain a single electron so that $L_3=0.5$. However, for a Ni(II) ($3d^8$) ion with the same crystal-field parameters, the lower doublet $|\psi_{1,2}\rangle$ would be completely filled by four electrons and the upper doublet $|\psi_{4,5}\rangle$ would be half filled by two electrons (both in the same spin state) so that $L_2=0$. Since the ratios $\gamma/|\alpha|$ and $\gamma'/|\alpha|$ will be different on the M(II) and M′(III) sites, L_2 and L_3 are independent of each other.

Because $\langle\psi_{1,2}|L_\pm|\psi_{1,2}\rangle=\langle\psi_{4,5}|L_\pm|\psi_{4,5}\rangle=0$, the matrix elements of $\mathbf{L}_2\cdot\mathbf{S}_2$ and $\mathbf{L}_3\cdot\mathbf{S}_3$ on the M(II) and M′(III) sites are diagonal with $\langle\psi_i;\sigma_2|\mathbf{L}_2\cdot\mathbf{S}_2|\psi_i;\sigma_2\rangle=\pm L_2\sigma_2$ and $\langle\psi_i;\sigma_3|\mathbf{L}_3\cdot\mathbf{S}_3|\psi_i;\sigma_3\rangle=\pm L_3\sigma_3$, where σ_2 and σ_3 are the z components of the spin for the M(II) and M(III)′ ions. So the eigenvalues of H_2 and H_3 are $\epsilon^{\pm}_{2\sigma_2}=(\pm\lambda_2L_2+3J_c\langle S_{3z}\rangle)\sigma_2$ and $\epsilon^{\pm}_{3\sigma_3}=(\pm\lambda_3L_3+3J_c\langle S_{2z}\rangle)\sigma_3$.

The magnetic moments $M_2(T)=\langle 2S_{2z}+L_{2z}\rangle$ and $M_3(T)=\langle 2S_{3z}+L_{3z}\rangle$ on the M(II) and M′(III) sites are evaluated self-consistently. The average magnetization is then given by $M_{\mathrm{avg}}(T)=(M_2(T)+M_3(T))/2$, where we adopt the convention

that $M_3(T)>0$. The magnetic moment $M_2(T)$ is obtained from the equations

$$\langle S_{2z}\rangle = \frac{2}{Z_2}\sum_{\sigma_2} \sigma_2 e^{-3J_c\langle S_{3z}\rangle\sigma_2/T}\cosh(\lambda_2\sigma_2 L_2/T), \tag{4}$$

$$\langle L_{2z}\rangle = -\frac{2L_2}{Z_2}\sum_{\sigma_2} e^{-3J_c\langle S_{3z}\rangle\sigma_2/T}\sinh(\lambda_2\sigma_2 L_2/T), \text{ and} \tag{5}$$

$$Z_2 = 2\sum_{\sigma_2} e^{-3J_c\langle S_{3z}\rangle\sigma_2/T}\cosh(\lambda_2\sigma_2 L_2/T). \tag{6}$$

Of course, $M_3(T)$ is obtained by switching $\lambda_2 \leftrightarrow \lambda_3$, $L_2 \leftrightarrow L_3$, $\sigma_2 \leftrightarrow \sigma_3$, and $\langle S_{2z}\rangle \leftrightarrow \langle S_{3z}\rangle$.

We evaluate the critical temperature T_c by linearizing $\langle S_{2z}\rangle$ and $\langle S_{3z}\rangle$, which results in the expression

$$\left(\frac{T_c}{J_c}\right)^2 = 9\frac{\sum_{\sigma_2}\sigma_2^2\cosh\left(\frac{\lambda_2\sigma_2 L_2}{T_c}\right)}{\sum_{\sigma_2}\cosh\left(\frac{\lambda_2\sigma_2 L_2}{T_c}\right)}\frac{\sum_{\sigma_3}\sigma_3^2\cosh\left(\frac{\lambda_3\sigma_3 L_3}{T_c}\right)}{\sum_{\sigma_3}\cosh\left(\frac{\lambda_3\sigma_3 L_3}{T_c}\right)}. \tag{7}$$

This relationship must be solved self-consistently for T_c/J_c, which appears on both sides of Eq. (7). In the limit $S_2=2$, $S_3=5/2$, and $L_3=0$, Eq. (7) reduces to an earlier result[8] for the Fe(II)Fe(III) bimetallic oxalates.

As $T\to T_c$ from below, M_2, M_3, and M_{avg} all vanish within MF theory as $(T_c-T)^{1/2}$. As $T\to 0$, $\langle S_{2z}\rangle \to -S_2$, $\langle S_{3z}\rangle \to S_3$, whereas $M_0 \equiv \lim_{T\to 0} M_{\text{avg}}(T)$ depends on the signs of λ_2 and λ_3. There are four possibilities:

$$M_0 = \begin{cases} \left(S_3-\frac{L_3}{2}\right)-\left(S_2-\frac{L_2}{2}\right); & \lambda_2>0, \quad \lambda_3>0 \\ \left(S_3+\frac{L_3}{2}\right)-\left(S_2+\frac{L_2}{2}\right); & \lambda_2<0, \quad \lambda_3<0 \\ \left(S_3+\frac{L_3}{2}\right)-\left(S_2-\frac{L_2}{2}\right); & \lambda_2>0, \quad \lambda_3<0 \\ \left(S_3-\frac{L_3}{2}\right)-\left(S_2+\frac{L_2}{2}\right); & \lambda_2<0, \quad \lambda_3>0. \end{cases}$$

To find the regions of MC, we use the conditions that either $M_{\text{avg}}(T)$ changes sign near T_c or $M_{\text{avg}}(T)$ vanishes at $T=0$.

MC regions are indicated in Fig. 2 for the family M(II)Mn(III) with M=Ni, Co, or Fe,[9] denoted by the labels 1, 2 and 3, respectively. Figure 3 shows MC regions 4 and 5 for the family V(II)M′(III) with M′=Cr or V, respectively. The straight lines bordering the MC regions indicate that $M_0=0$, which implies that the zero-temperature sublattice moments exactly cancel. The MC regions above and below these lines are classified by their saturation values, with $M_0>0$ (below) when $|M_3(0)|>|M_2(0)|$ and $M_0<0$ (above) when $|M_2(0)|>|M_3(0)|$. Curved boundaries indicate the onset of MC near T_c. Consequently, T_{comp} is small near the straight boundary and approaches T_c near the curved boundary.

In Fig. 2, the MC regions for Co(II) and Ni(II) have similar shapes but region 2 is shifted with respect to region 1 due to the larger spin $S_2=3/2$ for Co(II) compared to $S_2=1$ for Ni(II). Since Mn(III) has a spin of $S_3=2$ and both Co(II) and Ni(II) have negative values for λ_2 (implying that $\mathbf{L}_2$ and $\mathbf{S}_2$ tend to be parallel), a smaller value of L_2 is required for MC in the Co(II)Mn(III) compound. MC for Ni(II) and Co(II) occurs in regions 1a and 2a with $M_0>0$ and in regions 1b and 2b with $M_0<0$. In regions 1a and 2a with $M_0>0$, the Ni(II) and Co(II) moments are greater than the Mn(III) moment close to T_c; in regions 1b and 2b with $M_0<0$, the Mn(III) moment dominates close to T_c. In Fig. 4, we plot the average magnetization for Co(II)Mn(III) compounds with $L_2=0.5$ and $L_3=0.0$, 0.26, or 0.52, traversing region 2a. The MC regions are distributed in an odd fashion with respect to

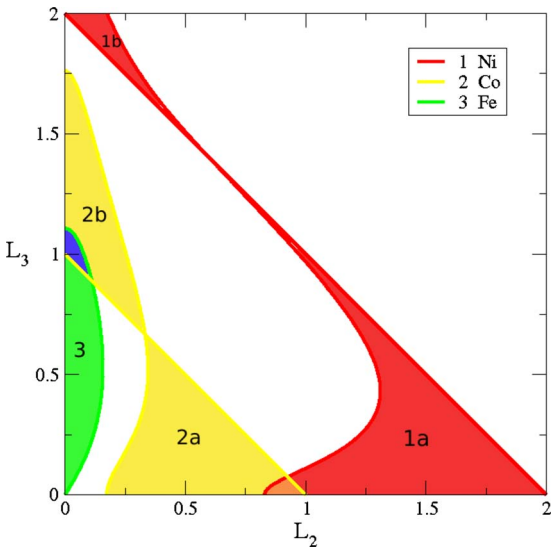

FIG. 2. (Color online) MC regions for the family M(II)Mn(III) with M=Ni (region 1), Co (region 2), or Fe (region 3) plotted as a function of the average orbital angular momenta L_2 and L_3.

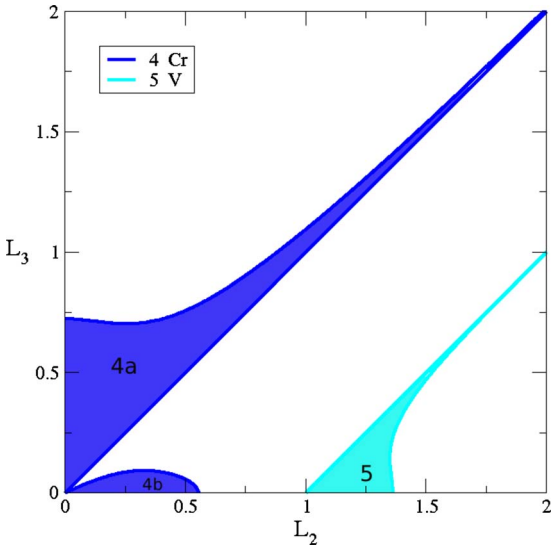

FIG. 3. (Color online) MC regions for the family V(II)M′(III) with M′=Cr (region 4) or V (region 5) plotted as a function of the average orbital angular momenta L_2 and L_3.

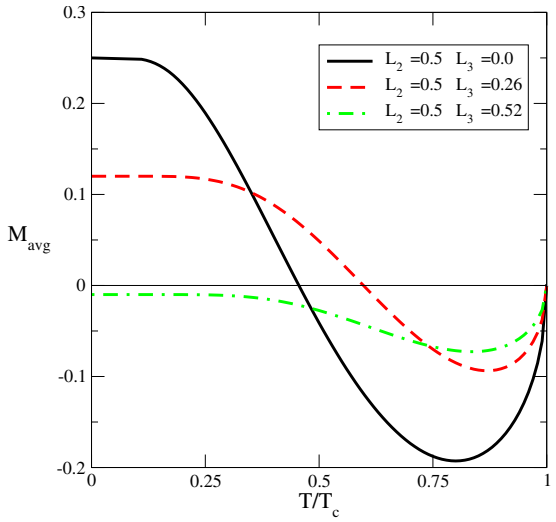

FIG. 4. (Color online) M_{avg} versus T/T_c for Co(II)Mn(III) compounds with $L_2=0.5$ and $L_3=0.0$ (solid), 0.26 (dashed), and 0.52 (dash-dotted), which traverse region 2a in Fig. 2.

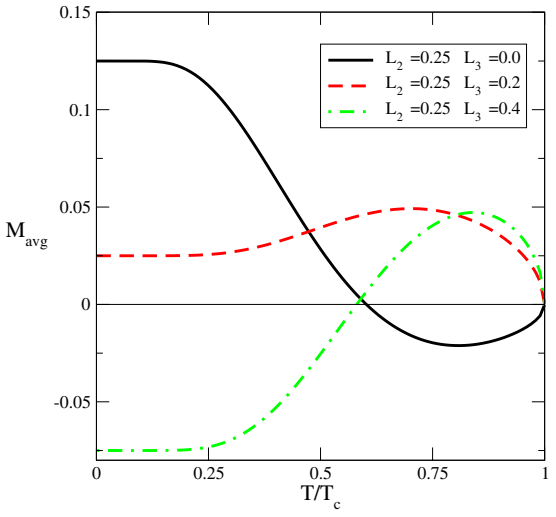

FIG. 5. (Color online) M_{avg} versus T/T_c for V(II)Cr(III) compounds with $L_2=0.25$ and $L_3=0.0$ (solid), 0.2 (dashed), and 0.4 (dot-dash), which traverse regions 4a and 4b in Fig. 3.

the $M_0=0$ line because λ_2 and λ_3 have opposite signs.

Because both Fe(II) and Mn(III) have the same spin $S_2=S_3=2$, MC region 3 for Fe(II) in Fig. 2 is restricted to small values of L_2. Since $M_0<0$, the Mn(III) moment (with $\lambda_3>0$ or antiparallel spin-orbit coupling) is greater than the Fe(II) moment (with $\lambda_2<0$ or parallel spin-orbit coupling) close to T_c. For larger values of L_2, the Fe(II) moment would always dominate over the Mn(III) moment.

Our results for the V(II)M′(III) series[10] are displayed in Fig. 3. Regions 4 and 5 have different shapes because Cr(III) has the same spin $S_3=3/2$ as V(II) with $S_2=3/2$, while V(III) has the smaller spin $S_3=1$. All of these ions have positive values for λ (see Table I), so $\mathbf{S}_i$ and $\mathbf{L}_i$ tend to be antiparallel. For V(II)Cr(III) compounds, the majority of the MC region (4a) occurs when $M_0<0$ and $L_3>L_2$ because $\lambda_3>\lambda_2$. As a result, the Cr(III) moment is usually larger than the V(II) moment close to T_c. In region 4b with $M_0>0$, a bubble of MC exists for small values of L_3, where the V(II) moment dominates the Cr(III) moment near T_c due to its stronger spin-orbit energy $\lambda_2 L_2 S_2>\lambda_3 L_3 S_3$. Figure 5 plots the average magnetization for V(II)Cr(III) compounds with fixed $L_2=0.25$ and $L_3=0.0$, 0.2, and 0.4, traversing regions 4a and 4b. Notice that MC is absent for $L_3=0.2$, which lies between regions 4a and 4b. For V(II)V(III) compounds, MC exists in region 5 only for small values of L_3 with $M_0>0$ so that the V(II) moment dominates near T_c.

We also investigated the series M(II)Ru(III) (M=Fe or Cu).[11] MC is absent due to the large spin-orbit coupling λ_3 of Ru(III) (see Table I) and the resulting low-spin state $S_3=1/2$ induced by the crystal-field potential. For Fe(II)Ru(III) compounds with $S_2=2$, the Fe(II) moment is always much larger than the Ru(III) moment despite the large spin-orbit coupling of Ru(III). For Cu(II)Ru(III) compounds, the spins on the two sublattices are identical with $S_2=S_3=1/2$. Because λ_2 and λ_3 have approximately the same magnitudes but opposite signs, the Cu(II) moment remains larger than the Ru(III) moment for all temperatures and for all values of L_2 and L_3. Hence, the magnetic moments of Fe(II) and Cu(II) always dominate in the family M(II)Ru(III).

Generally, MC occurs because the ion with the smaller saturation moment but stronger spin-orbit coupling initially orders more rapidly with decreasing temperature than the ion with the larger saturation moment. As demonstrated by region 3 of Fig. 2 near $L_2=0$ and by region 4b of Fig. 3 near $L_3=0$, MC can even occur when $S_2=S_3$ and with antiparallel spin-orbit coupling ($\lambda_i>0$) between $\mathbf{S}_i$ and $\mathbf{L}_i$, despite the smaller saturation moment $|2S_i-L_i|$, due to the stronger initial ordering of the spin $\mathbf{S}_i$. Without spin-orbit coupling, the ion with the larger saturation moment would always dominate over the ion with the smaller saturation moment.

The MC regions in Figs. 2 and 3 result from the interplay between S_2, S_3, L_2, L_3, λ_2, and λ_3. When $M_3(T)$ orders more rapidly below T_c but $|M_2(0)|>|M_3(0)|$, MC appears in regions 1b, 2b, 3, and 4a. When $M_2(T)$ orders more rapidly below T_c, but $|M_3(0)|>|M_2(0)|$, MC appears in regions 1a, 2a, 4b, and 5. The relative magnitude of λ_2 or λ_3 changes the sizes of the MC regions but not their overall placement; compare the sizes of regions 1a and 1b. By contrast, the placement of the MC regions in Figs. 2 and 3 are primarily determined by S_2, S_3, L_2, and L_3.

Experiments reveal that the deviation in the paramagnetic susceptibility χ from its spin-only value[5,9,10] is relatively small. For example, the Curie constant C for a Fe(II)Mn(III) compound is about 30% higher than its spin-only value.[9] This implies that there is a small but nonzero orbital contribution to the magnetic moment.[16] Earlier work[8] indicated that Fe(II)Fe(III) compounds which exhibit MC have values of L_2 just above the threshold of 0.25. Correspondingly, in the families of ferrimagnetic compounds studied here, L_2 and L_3 are probably smaller than 1. We conclude that MC is most likely in the compounds Fe(II)Mn(III), Co(II)Mn(III), and V(II)Cr(III): see regions 2a, 3, 4a, and 4b in Figs. 2 and 3. On the other hand, MC is less likely in the compounds Ni(II)Mn(III) and V(II)V(III), where larger values of L_2 and L_3 are required for MC in regions 1 and 5.

In contrast to the wide range of cations that have been used in the synthesis of Fe(II)Fe(III) bimetallic oxalates,[4]

only the single cation $A=N(n\text{-}C_4H_9)_4$ has been employed in the synthesis of Fe(II)Mn(III), Co(II)Mn(III), and V(II)Cr(III) compounds.[9,10] While this cation is associated with MC in the Fe(II)Fe(III) oxalates, there is no guarantee that it will also produce MC in other ferrimagnetic compounds. Therefore, it may be worth investigating Fe(II)Mn(III), Co(II)Mn(III), and V(II)Cr(III) compounds with some of the other cations that produce MC in the Fe(II)Fe(III) oxalates such as $A=N(n\text{-}C_5H_{11})_4$, $N(C_6H_5CH_2)(n\text{-}C_4H_9)_3$, $(C_6H_5)_3PNP(C_6H_5)_3$, $P(n\text{-}C_4H_9)_4$, $CoCp_2^*$, and $FeCp_2^*$. We are hopeful that at least some of these compounds will yield values of L_2 and L_3 associated with MC in Figs. 2 and 3.

This paper has investigated the possibility of MC in several families of bimetallic oxalates that exhibit AF interactions between transition metals M(II) and M′(III). For certain cations, MC may be possible within the families of M(II)Mn(III) and V(II)M′(III) bimetallic oxalates but is not possible within the family of M(II)Ru(III) compounds. We hope that future experiments will continue to explore the phenomenon of MC in this fascinating class of molecule-based magnets.

Research was sponsored by NSF Grant Nos. DMR-0548011, OISE-0730290 and EPS-0447679 (ND EPSCoR), by the Laboratory Directed Research and Development Program of Oak Ridge National Laboratory, managed by UT-Battelle, LLC for the U. S. Department of Energy under Contract No. DE-AC05-00OR22725, and by the Division of Materials Science and Engineering of the U.S. DOE.

[1] H. Tamaki, Z. J. Zhong, N. Matsumoto, S. Kida, M. Koikawa, N. Achiwa, Y. Hashimoto, and H. Õkawa, J. Am. Chem. Soc. **114**, 6974 (1992).

[2] See, the review R. Clément, S. Decurtins, M. Gruselle, and C. Train, Monatsch. Chem. **134**, 117 (2003), and references therein.

[3] C. Mathonière, S. G. Carling, D. Yusheng, and P. Day, J. Chem. Soc., Chem. Commun. **1994**, 1551.

[4] C. Mathonière, C. J. Nuttall, S. G. Carling, and P. Day, Inorg. Chem. **35**, 1201 (1996).

[5] C. J. Nuttall and P. Day, Chem. Mater. **10**, 3050 (1998).

[6] E. Coronado, J. R. Galán-Mascarós, C. J. Gómez-García, and J. M. Martinez-Agudo, Adv. Math. **11**, 558 (1999); E. Coronado, J. R. Galán-Mascarós, C. J. Gómez-García, J. Ensling, and P. Gütlich, Chem.-Eur. J. **6**, 552 (2000).

[7] G. Tang, Y. He, F. Liang, S. Li, and Y. Huang, Physica B (Amsterdam) **392**, 337 (2007).

[8] R. S. Fishman and F. A. Reboredo, Phys. Rev. Lett. **99**, 217203 (2007); Phys. Rev. B **77**, 144421 (2008).

[9] E. Coronado, J. R. Galán-Mascarós, and C. Martí-Fastaldo, J. Mater. Chem. **16**, 2685 (2006).

[10] K. S. Min, A. L. Rhinegold, and J. S. Miller, Inorg. Chem. **44**, 8433 (2005).

[11] J. Larionova, B. Mombelli, J. Sanchiz, and O. Kahn, Inorg. Chem. **37**, 679 (1998).

[12] E. Coronado, J. R. Galán-Mascarós, C. J. Gómez-García, and V. Laukhin, Nature (London) **408**, 447 (2000).

[13] M. Clemente-León, E. Coronado, J. R. Galán-Mascarós, and C. J. Gómez-García, Chem. Commun. (Cambridge) **1997**, 1727.

[14] In most 3d and 4d bimetallic oxalates, the orbital-correlation energy is weak, so the total orbital angular momentum L_t of the electrons is not a good quantum number and Hund's second rule is not obeyed. Even if L_t is a good quantum number, however, the formalism developed in this paper can still be employed because the C_3-symmetric crystal-field potential will split the $L_t=2$ ($3d^n$, $n=1$, 4, 6, or 9) or $L_t=3$ ($n=2$, 3, 7, or 8) multiplets into a sequence of singlets and doublets.

[15] B. Bleaney and K. W. H. Stevens, Rep. Prog. Phys. **16**, 108 (1953).

[16] O. Kahn, *Molecular Magnetism* (VCH, New York, 1994).